Studying the impurity charge and main ion mass dependence of impurity confinement in ECR-heated TJ-II stellarator plasmas

B. Zurro[1], E.M. Hollmann[2], A. Baciero[1], M.A. Ochando[1], K.J. McCarthy[1], F. Medina[1], J. L. Velasco[1], I. Pastor[1], D. Baião[3], E. de la Cal[1], D. Rapisarda[1] and TJ-II team[1]

[1]*Laboratorio Nacional de Fusión, CIEMAT, Madrid, Spain*

[2]*University of California-San Diego, La Jolla, CA, USA*

[3]*Instituto de Plasmas e Fusão Nuclear, Instituto Superior Técnico, Universidade de Lisboa, 1049-001 Lisbon, Portugal*

INTRODUCTION. The simultaneous attainment of short impurity and long energy confinement times is crucial for obtaining relevant magnetically-confined nuclear fusion plasmas [1]. In the case of stellarators, a critical issue is the increasing impurity confinement time at high densities, which can lead to impurity accumulation and radiative collapse [2].

In tokamaks the influence of ion charge, Z, on impurity transport was studied in ASDEX Upgrade [3] and in JET [4] by gas puffing. In contrast, in LHD [5] the charge dependence on impurity confinement was investigated by injecting pellets of C, Al or Ti. In previous work in TJ-II, laser blow-off injection (LBI) of BC, LiF, and Fe was used to study impurity confinement in electron cyclotron resonance (ECR) heated plasmas [6]. In this work, the dependence of impurity confinement time on the charge and mass of the impurity ions injected from LiF, BN, and W is reported.

EXPERIMENTAL RESULTS AND DISCUSSION. TJ-II is a four-period, low magnetic shear stellarator with major and averaged minor radii of 1.5 m and ≤0.22 m, respectively. Central electron densities and temperatures up to 1.7×10^{13} cm^{-3} and 1 keV respectively can be achieved for plasmas created and maintained by ECRH at the second harmonic (f = 53.2 GHz, $P_{ECRH} \leq 500$ kW). The magnetic field is generated by poloidal, toroidal and vertical field coils, and the resultant plasma cross-section is bean shaped with on-axis magnetic field, $B(0) \leq 1$ T. Wall conditioning is performed with lithium coating on the inner vacuum vessel walls and a short helium glow discharge prior to operation [7].

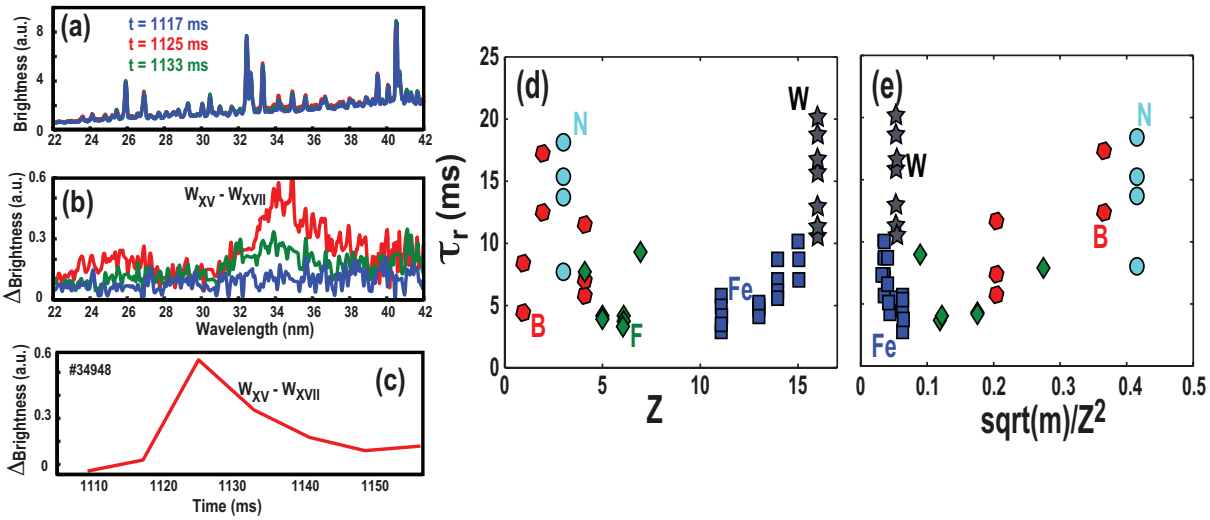

Fig. 1. VUV spectra following W injection showing: (a) spectra at three different time steps, (b) difference spectra obtained by subtracting a background spectrum obtained prior to injection, and (c) time behaviour of W XV – XVII continuum brightness, d-e) global confinement times for different species and charge states.

An overview of global impurity confinement times obtained with LiF, BN and W is shown in Figs. 1 and 2. VUV lines are used to track individual charge states. In the case of W injection, individual VUV emission lines are not observed, instead a weak broadband continuum spectrum, between ≈25 and ≈40 nm, is seen, as shown in Fig. 1(a). This continuum structure is associated with W charge states from XV to XVII [8]. Overall, a trend towards longer confinement of higher charge states is noted. This could be interpreted as the higher charge states have slower radial transport or as radially broader emission zones. Surprisingly, there are some long confinement points at $Z = 2$. It is worth noting that the ion root is predicted at the edge, $\rho > \approx 0.8$ [9]. For comparison, the global energy confinement time τ_E [10] is typically about 2 ms for the density range studied here.

In these low-density, low-ion-temperature plasmas, impurities are in the collisional regime and their neoclassical radial diffusion is expected to be proportional to collisionality, giving confinement times $\tau \propto \sqrt{m} / Z^2$. Fig. 1(e) shows measured confinement times as a function of $\sqrt{m} / Z^2$, indicating that this scaling is not well followed by the data. It should be noted that radial variation in E_r could complicate interpretation of global confinement times.

In order to focus on central impurity confinement, decay times of central chord SXR data is plotted in Fig. 2(a) as a function of the line-averaged electron density for the three samples for similar discharges. The data show clear differences in decay times that increase from ≈4 ms for LiF injection, to 6 ms for BN and up to ≈ (10 ± 3) ms for W injection. The trend observed here suggests that at higher densities the difference between the confinement times of the light and heavy impurities tends to narrow. A possible explanation for this could

be that the reduction of transport coefficients due to larger $Z{\cdot}E_r$ is stronger than the correspondingly larger thermo-dynamical force.

In addition to the central SXR confinement times, an effort was made to study the radial dependence of impurity confinement. The impurity confinement times at different SXR chords, are plotted in Fig. 2(b). It can be seen that confinement times tend to increase from the centre outwards.

Similar analysis was performed with bolometer view chords, which are more sensitive to the plasma edge [11]. Typical results are shown in Fig. 2(c). It can be seen that there is still a clear mass/charge dependence in the plasma core; this is not as clear at the plasma periphery. These results may be again indicative of the important role of the radial electric field. For low-density TJ-II plasmas, E_r is larger in the core, hence differences in confinement transport caused by its Z dependency should be larger there than in outer regions where E_r is closer to zero [12].

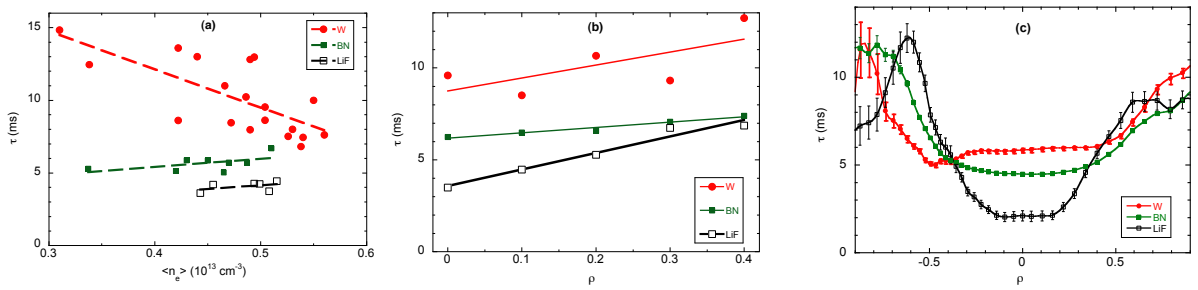

Fig. 2. (a) Influence of the mass/charge of the injected impurity on the decay time relaxation for a central collimated X-ray detector. An increase in confinement time with mass and expected charge of the central ions is seen when data are plotted as a function of n_e, (b) behaviour of the decay time of different soft X-ray channels for injected LiF, BN and W and for four impact parameters of the chord ranging from $\rho = 0$ to 0.4, (c) decay time of local bolometer signals versus normalized radius for injected LiF, BN and W. Note: decay is fastest in central radii, corresponding to higher charge states.

Toroidal impurity transport measurements. In these experiments impurities are injected at a single toroidal location, therefore impurity ion toroidal transport can be investigated. The AXUV arrays [13] have sufficiently high temporal resolution for this, as toroidal transport times are of order ~1 ms. Total radiated power estimated at different toroidal locations by the AXUV arrays following B_4C injection is shown in Fig. 3(a). It can be seen that the radiation remains dominantly localized near the injection port, at $\phi = 90°$, but spreads toroidally on a timescale of ~ 1 ms in a semi-diffusive manner (i.e. without a clear preferential flow direction). Fig. 3(b) shows an example of toroidal transport of impurity emission following tungsten injection. In this case, a preferential toroidal flow of the impurities can be seen. The measured toroidal flow is in the main ion core rotation direction (clockwise) at about 5 km/s,

close to the measured core rotation velocity of about 10 km/s. The measured flow has a high Mach number form, with much higher directed velocity than parallel spreading velocity. This high Mach number flow is indicative of flow entrainment in the background bootstrap rotation, rather than a self-generated bootstrap flow (which would result in a low Mach number flow).

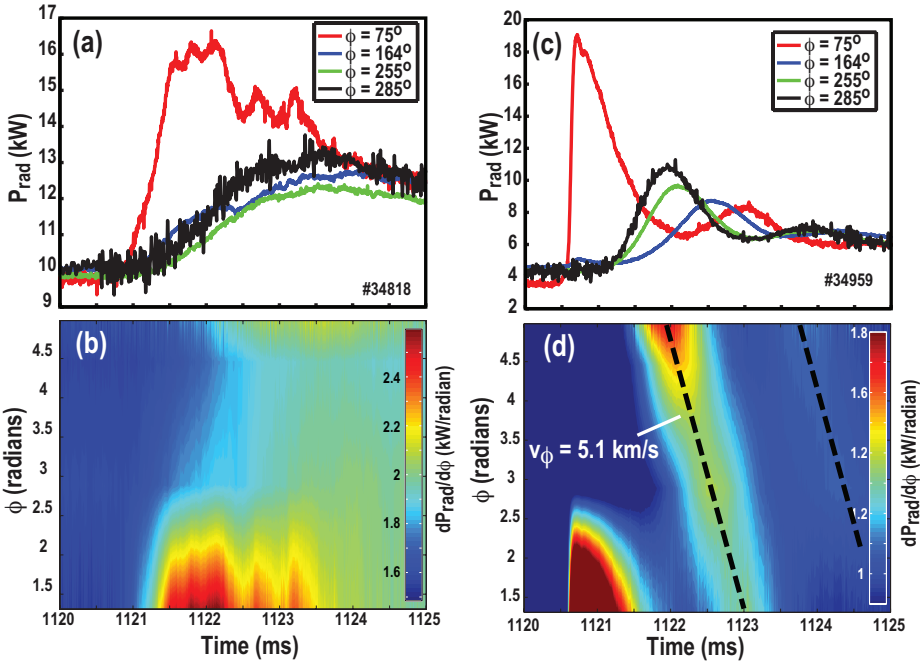

Fig. 3. (a) Toroidal transport of impurities following B_4C injection showing: (a) time traces of radiated power at different toroidal angle ϕ, (b) same data but converted to contour plot vs ϕ and time. Injection occurs at 1120 ms, (c) toroidal transport of impurities following W injection showing and (d) time traces of radiated power at different toroidal angle (ϕ), (d) same data but converted to contour plot versus ϕ and time.

Acknowledgements. This work was partially funded by the Spanish "Ministerio de Economía y Competitividad" under Grants No. ENE2009-10181, ENE2010-19109, ENE2010-19676 and ENE2012-30832, and by the US Department of Energy under DE-FG02-07ER54917. This project has received funding from the European Union's Horizon 2020 research and innovation programme under grant agreement number 633053. The views and opinions expressed herein do not necessarily reflect those of the European Commission.

References

[1] Whyte DG *et al* 2010 *Nucl. Fusion* **50** 105005
[2] Burhenn R *et al* 2009 *Nucl. Fusion* **49** 065005
[3] Dux R *et al* 1999 *Nucl. Fusion* **39** 11 1509-1522
[4] Giroud *C et al* 2007 *Nucl. Fusion* **47** 313-330
[5] H. Nozato *et al* 2004 *Phys. Plasmas* **5** 1920
[6] Zurro B, Hollmann E, Baciero A *et al* 2011 *Nucl. Fusion* **51** 062015
[7] Sánchez J, Tabarés F, Tafalla D *et al* 2009 *J. Nucl. Materials* **390** 852
[8] Peacock NJ *et al* 2008 *Can. J. Phys.* **86** 277
[9] Velasco JL *et al* 2011 *Plasma Phys. Control. Fusion* **53** 11 115014
[10] Ascasíbar E *et al* 2005 *Nucl. Fusion* **45** 276
[11] Zurro B, Baciero A *et al* 2004 *Rev. Sci. Instrum.* **75** 104231
[12] Arévalo J *et al* 2013 *Nucl. Fusion* **53** 023003
[13] Ochando MA 2006 *Fusion Sci. & Tech.* **50** 313